European Review for Medical and Pharmacological Sciences 2019; 23: 4908-4916

Role and mechanism of microRNA-548c-3p/c-Myb in myocardial infarction fibrosis in rats

L.-X. ZHANG[1], S.-H. ZHANG[1], C.-Q. WANG[2], Q. BING[3], Z. ZHAO[3], J. WANG[3], L. ZHANG[3]

[1]Department of Gerontology, The Third Hospital of Hebei Medical University, Shijiazhuang, China
[2]Department of Cardiology, The Third Hospital of Hebei Medical University, Shijiazhuang, China
[3]Department of Neuromuscular Disease, The Third Hospital of Hebei Medical University, Shijiazhuang, China

Lixuan Zhang and Shenghan Zhang contributed equally to this work

Abstract. – OBJECTIVE: To investigate the role of micro ribonucleic acid (miR)-548c-3p in myocardial fibrosis after myocardial infarction (MI), and to explore the possible underlying.

MATERIALS AND METHODS: The rat model of MI was successfully established *in-vivo*. MiR-548c-3p was upregulated via lentivirus transfection with miR-548c-3p mimics. Cardiac function of rats was detected via echocardiography. Meanwhile, Sirius red and Masson staining were used to detect the level of fibrosis index in MI model. Subsequently, myocardial fibroblasts were isolated and cultured *in vitro*. An oxygen-glucose deprivation (OGD) model was established to mimicking the ischemic condition. Furthermore, the relationship between miR-548c-3p and c-Myb was verified, and the levels of fibrosis-related factors (including α-SMA and COL1A1) were measured.

RESULTS: *In-vivo* experiments showed that miR-548c-3p expression in rats was significantly down-regulated at 2 and 4 weeks after MI. Up-regulation of miR-548c-3p significantly improved cardiac function, reduced myocardial fibrosis and inhibited the protein expression of proto-oncogene c-Myb (c-Myb). *In vitro* experiments revealed that c-Myb was a target gene of miR-548c-3p. In addition, miR-548c-3p could inhibit the expressions of α-SMA and COL1A1 through targeting c-Myb.

CONCLUSIONS: MiR-548c-3p could improve myocardial fibrosis by targeting c-Myb.

Key Words:
MicroRNA-548c-3p (miR-548c-3p), Proto-oncogene c-Myb (c-Myb), Myocardial infarction (MI), Fibrosis.

Introduction

Cardiovascular disease is still one of the important causes of death worldwide, whose mortality rate is far higher than that of other diseases. Meanwhile, the morbidity rate of cardiovascular diseases has shown an increasing trend year by year[1]. Myocardial infarction (MI) is known as an important fatal cardiovascular disease. The pathogenesis of MI is that ruptured coronary atherosclerotic plaques block the lumen or cause secondary thrombus, leading to persistent ischemia and hypoxia of the coronary artery. Ultimately, myocardial tissue necrosis occurs. Moreover, the morbidity rate of MI is increasing year by year, seriously threatening human health and quality of life[2]. Due to rapid development of molecular biology, the exploration of micro ribonucleic acid (miRNA) and MI has been facilitated in recent years[3,4]. Existing results have demonstrated that the pathophysiological development of MI significantly affects the expression of miRNAs in the peripheral blood of MI patients. This reveals the severity of MI and coronary artery lesions[5,6]. At the same time, miRNA inhibits myocardial apoptosis and regulates the reprogramming of cardiac fibroblasts into myocardial cells[7-9]. MiRNAs are a kind of small non-coding RNAs in eukaryotes with about 21-25 nt in length. Previous studies have indicated that miRNAs are involved in regulating gene expression based on base complementary binding to mRNAs (including target sequences)[10,11]. Generally, hundreds of mRNA targets have been found for miRNAs. Meanwhile, different targets are likely to display multiple functions in a specific pathway. Therefore, miRNAs potentially affect the expression of all signaling pathways, thereby playing a dominant role in cellular metabolism in multiple species. In addition, miRNAs have exhibited several functions of cell differentiation and metabolism by inhibition of target genes during cellular evolution process.

Corresponding Author: Li Zhang, MD; Ph.D; e-mail: daylight1981@126.com

Furthermore, such functions are usually indispensable[11]. As a key in understanding the complex and hidden pathogenesis of diseases, miRNAs have attracted increasingly more attention. For example, as a member of the miRNA family, miR-548c-3p is widely existed in different species. Studies have confirmed that miR-548c-3p plays an important biological role in the body. Moreover, miR-548c-3p has become a new breakthrough point from the perspective of the formation, evolution, diagnosis and prognosis of diseases[12-16]. Therefore, studying the role of miR-548c-3p is of great significance in revealing the regulatory mechanism of gene expression, as well as the prevention and treatment of diseases. In this study, the expression of miR-548c-3p in myocardial fibrosis after MI was detected. Furthermore, its exact role in MI as well as the possible underlying mechanism was investigated.

Materials and Methods

Establishment of the MI Model in Rats

Male adult Sprague-Dawley (SD) rats weighing 200-250 g aged 8-10 weeks old were purchased from Hebei Medical University Animal Center. All rats were fed under ambient temperature of (25±2)°C and 12/12 h lighting condition. After adaptive feeding for 1 week before modeling, all rats were used for subsequent experiments in accordance with the Laboratory Animal Management Regulations and Animal Ethical Requirements. This study was approved by the Animal Ethics Committee of Hebei Medical University Animal Center.

The rats were anesthetized *via* intraperitoneal injection of 100 g/L chloral hydrate (3 mL/kg). After that, they were fixed on the operating table in a supine position. According to the literature, the chest was opened between the left 3rd and 4th intercostal spaces, followed by exposure of the heart. The pericardium was opened. Then, a needle was inserted at 3 mm below the root of left auricle and withdrawn from the cone edge of the pulmonary artery. The left anterior descending coronary artery (LAD) was ligated with 5-0 sutures. If the ventricular muscle below the ligature site turned pale or white, the ventricular wall motion declined, and there were led II ECG T-wave peak and ST-segment arch elevation, the model was successfully established. In the experiment, all rats were divided into 4 groups, including: sham group (n=15, LAD was not ligated, and the remaining operations were the same as those in MI group), MI group (n=15), MI + miR-NC group (n=6, after LAD was ligated, the mixture of 20 μL negative control mimics and Lipofectamine 2000 (Invitrogen, Carlsbad, CA, USA) was injected into the left ventricular anterior wall below the ligature site using insulin pen) and MI + miR-NC group (n=15, after LAD was ligated, the mixture of 20 μL miR-548c-3p mimics and Lipofectamine 2000 was injected into the left ventricular anterior wall below the ligature site). Finally, the chest was sutured layer by layer, and penicillin (200,000 U/rat) was administrated for anti-infective therapy for 3 d after operation.

Quantitative Real-Time Polymerase Chain Reaction (qRT-PCR)

14 d and 28 d after surgery, 3 rats in each group were sacrificed for miRNA detection. Total RNA in tissues and cells was extracted according to the instructions of TRIzol Reagent (Invitrogen, Carlsbad, CA, USA). TaqMan miRNA assay (Applied Biosystems, Foster City, CA, USA) was used to measure the expression of miR-548c-3p normalized to miRNA U6. Primer sequences used in this study were as follows: miR-548c-3p, F: 5'-CACCAGGACCGTCCTTACTC-3', R: 5'-GCTAGGTGTCCGAGATAGGA-3'; U6: F: 5'-GCTTCGGCAGCACATATACTAAAAT-3', R: 5'-CGCTTCAGAATTTGCGTGTCAT-3'.

Cardiac Function and Histology

At 28 d after surgery, 6 rats in each group were first taken and anesthetized. After that, M-mode ultrasound images were taken at the parasternal left ventricular long axis view using a small animal ultrasonic probe (model: Veno2100). Subsequently, the left ventricular end-systolic diameter and left ventricular end-diastolic diameter were determined, and EF and FS were calculated. Myocardial tissues in the infarction region were first collected from rats in 3 groups. After washing, the tissues were fixed in 40 g/L paraformaldehyde for 1 d, embedded in paraffin routinely and sliced into sections. Then staining was performed according to the instructions of kits (HE, Boster, Wuhan, China), followed by photography. Finally, morphology, collagen volume fraction and myocardial apoptosis were determined.

Western Blot Analysis

Myocardial tissues in the infarction border zone and cells after oxygen-glucose deprivation (OGD) treatment were selected for protein determination. Radioimmunoprecipitation assay (RIPA) tis-

sue lysate (Beyotime, Shanghai, China) was first added into tissues and cells. After homogenate and centrifugation, the protein supernatant was extracted. The concentration of extracted protein was determined using bicinchoninic acid (BCA) method (Pierce, Rockford, IL, USA). 20 μg protein was separated by 6% sodium dodecyl sulfate polyacrylamide gel electrophoresis (SDS-PAGE) and transferred onto polyvinylidene difluoride (PVDF) membranes (Millipore, Billerica, MA, USA). After sealing with 5% skimmed milk at room temperature for 2 h, the membranes were incubated with primary antibodies of c-Myb, COL1A1, α-SMA (α-smooth muscle actin) and GAPDH (glyceraldehyde 3-phosphate dehydrogenase) at 4°C overnight. After washing, the membranes were incubated with corresponding horseradish peroxidase (HRP)-labeled secondary antibody at room temperature for 1 h. Color development was performed *via* chemiluminescence instrument, followed by analysis *via* Image-J software (NIH, Bethesda, MD, USA). GAPDH was used as an internal reference.

Cell Culture

Neonatal Sprague-Dawley (SD) rats aged 1-2 days old were taken, disinfected with 75% ethanol and executed. Heart tissue was removed on the aseptic table, and connective and atrial tissues were removed. Ventricular tissues were cut into pieces (1 mm^3), and the cells were digested and separated with 0.25% trypsin. All cells were cultured in Dulbecco's Modified Eagle's Medium (DMEM) (Gibco, Rockville, MD, USA) containing 10% fetal bovine serum (FBS) (Gibco, Rockville, MD, USA), and maintained in an incubator with 5% CO_2 at 37°C for 60-90 min. Cardiac fibroblasts were obtained by differential adhesion method. After that, they were continued to culture in an incubator with 5% CO_2 at 37°C, followed by passage once after 1-2 d. Cells in the 2^{nd}-4^{th} generations were used for subsequent experiments.

Cell Transfection and Treatment

Cardiac fibroblasts were first pre-cultured in a 24-well plate for 24 h. After that, three groups were established to investigate the potential relationship between miR-548c-3p and cardiac fibroblasts, including: NC group (negative control), miR-548c-3p mimics (cardiac fibroblasts transfected with miR-548c-3p mimics) and mimics + c-Myb (cardiac fibroblasts transfected with miR-548c-3p mimics and Lv-Myb). All the stuff was purchased from RiboBio (Guangzhou, China). Cell transfection was performed according to the manufacturer's instructions of Lipofectamine RNAiMAX (Life Technologies, Gaithersburg, MD, USA). After culture for another 24 h, an oxygen-glucose deprivation (OGD) model was established to mimicking the ischemic condition[17]. OGD was performed by placing plates containing cardiac fibroblasts in serum-free DMEM in an anaerobic chamber (BD Anaerobe Pouch System, Franklin Lakes, NJ, USA). After incubation for 8 h at 37°C, the cells were collected for further analysis.

Luciferase Reporter Gene Assay

TargetScan, miRDB and microRNA predicted that c-Myb was the most likely target gene of miR-548c-3p. The wild-type c-Myb 3'-untranslated region (3'-UTR) gene was obtained *via* PCR amplification. Meanwhile, c-Myb 3'-UTR seed sequence AUUUUU was mutated to UGCUAU in strict accordance with a point mutation kit, thus obtaining mutant-type c-Myb 3'-UTR gene. Then, wild-type and mutant-type c-Myb 3'-UTR gene fragments were cloned into luciferase reporter vector to form luciferase reporter plasmid. Cardiac fibroblasts were first inoculated into 6-well plates at a density of 1×10^5 cells/well. Subsequently, Lipofectamine 2000, 500 μg c-Myb 3'-UTR or mutant-type c-Myb 3'-UTR plasmid was co-transfected with miR-548c-3p mimics or negative control sequences into cardiac fibroblasts. After incubation for 18 h, the cells were transferred into new 96-well plates. 24 h later, the cells were collected, and relative luciferase activity was detected.

Statistical Analysis

Statistical Product and Service Solutions (SPSS) 22. 0 software (IBM, Armonk, NY, USA) was used for all statistical analysis. Data were represented as mean ± SD (Standard Deviation). *t*-test was used for comparison of measurement data. One-way analysis of variance (ANOVA) was used to compare the difference among different groups, followed by Post-Hoc Test LSD (Least Significant Difference). $p<0.05$ was considered statistically significant.

Results

MiR-548c-3p was Down-Regulated During MI

Four different treatment groups were first established to detect the changes of miR-548c-3p expres-

sion. Compared with control group, the expression of miR-548c-3p in the MI area of MI group was significantly reduced. It was noteworthy that the expression of miR-548c-3p tended to decrease further over time. In transfection groups, we first excluded the effect of transfection plasmid on miR-548c-3p expression. Results indicated that miR-548c-3p mimics transfection significantly increased the expression of miR-548c-3p in MI region. This confirmed transfection efficiency of miR-548c-3p mimics (Figure 1). Furthermore, we removed the empty plasmid group in subsequent experiments.

MiR-548c-3p Improved Cardiac Function After MI

4 weeks later, LVEF and LVFS were measured in rats to assess cardiac function. Results demonstrated that the cardiac function of rats in MI group was significantly weaker than that of Sham group. Meanwhile, the cardiac function of rats over-expressing miR-548c-3p was significantly better than that of MI group after MI operation (Figure 2).

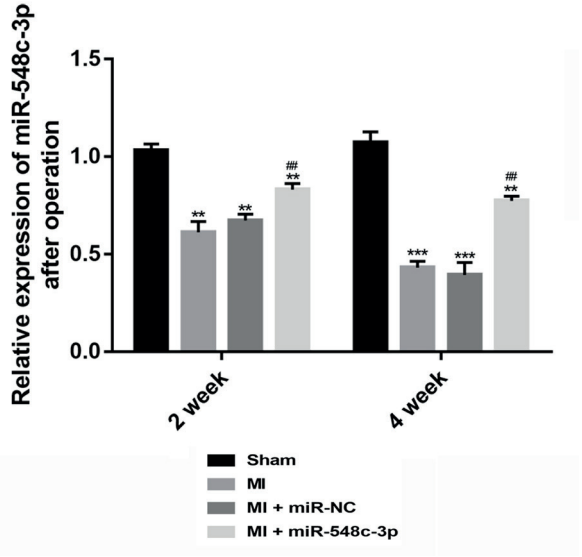

Figure 1. The expression of miR-548c-3p in myocardium border zone after infarction. (**p<0.01, ***p<0.0001 compared with Sham group, ##p<0.01 *vs.* MI group).

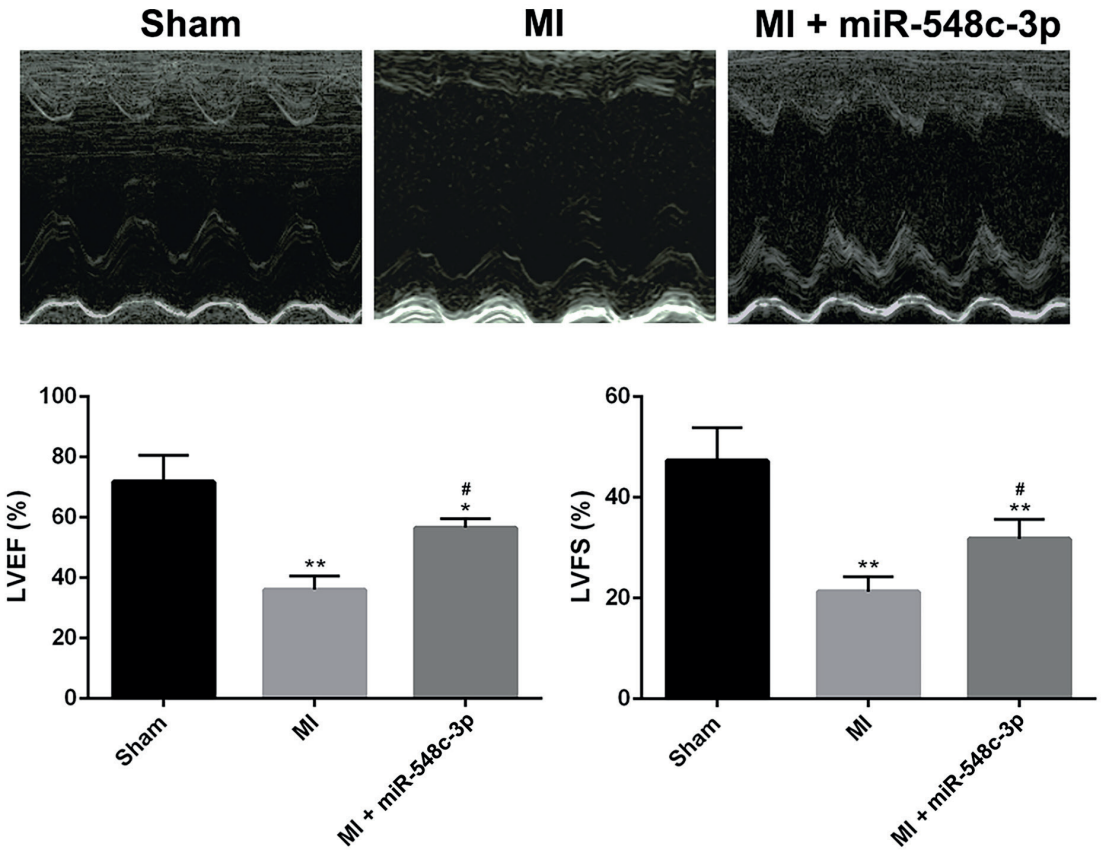

Figure 2. Up-regulation of miR-548c-3p improved cardiac function after infarction. ***A,*** Representative transthoracic M-mode echocardiograms from each group. ***B,*** and ***C,*** Statistical analysis of data obtained or derived from original echocardiographic records. Data were represented as means ± standard deviations. (*p<0.05, **p<0.01 compared with Sham group, #p<0.05 *vs.* MI group).

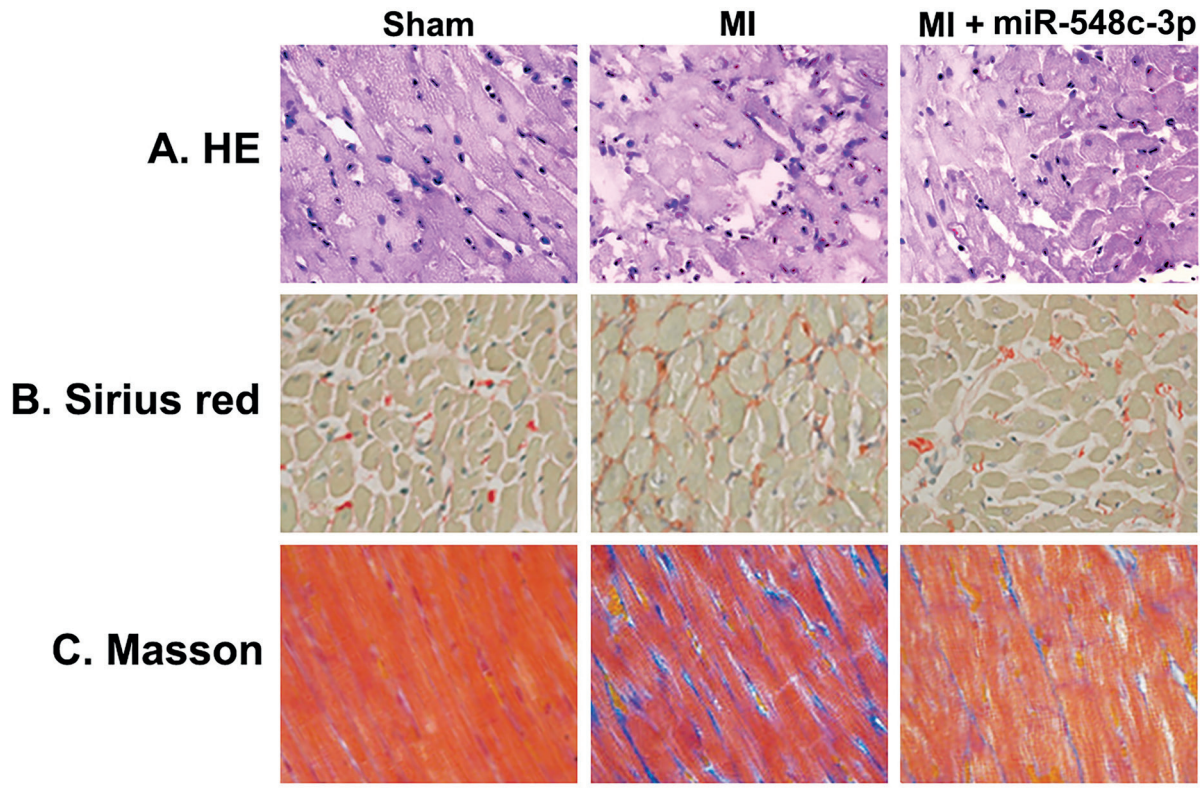

Figure 3. Up-regulation of miR-548c-3p stabilized heart structure and reduced myocardial fibrosis. Images of the myocardium and interstitial fibrosis stained with hematoxylin-eosin, Sirius red Masson after infarction (x200).

MiR-548c-3p Stabilized Heart Structure After MI

Myocardial tissues of rats treated with MI showed obvious structural damage. Cell edema, inflammatory cell infiltration and a large number of necrosis areas were reflected by HE staining (Figure 3). MiR-548c-3p could significantly ameliorate the pathological changes caused by MI treatment, showing excellent performance in stabilizing the structure of myocardial tissues.

MiR-548c-3p Reduced Myocardial Fibrosis After Infarction

Collagen volume fraction in myocardial tissues was measured by Masson and Sirius red staining. Results illustrated that Sham group showed the lowest collagen volume fraction. However, compared with MI group, miR-548c-3p mimics transfection could remarkably reduce collagen deposition in the myocardium of rats after MI (Figure 3, 4).

C-Myb was a target gene of miR-548c-3p

To elucidate the putative and possible targets of miR-548c-3p, we checked three publicly available algorithms, including: TargetScan, miRDB and microRNA. Results predicted that c-Myb was a supposed target of miR-548c-3p (Figure 5A). Subsequent luciferase reporter gene assay showed that lentivirus transfected with miR-548c-3p significantly reduced the fluorescence expression of wild-type-c-Myb. However, the fluorescence expression of mutant type-c-Myb was not significantly reduced. This indicated that c-Myb was a target gene of miR-548c-3p (Figure 5A). Based on the above finding, we found that the protein expression of c-Myb in myocardial tissues after 4 weeks of MI was significantly higher than that of sham-operated group. Consistent with our hypothesis, the expression of c-Myb in myocardial tissues after MI was significantly decreased by intervention of miR-548c-3p (Figure 5B).

In-Vitro Study Results

It was not surprising that transfection with miR-548c-3p mimics could significantly reduce the protein levels of c-Myb in myocardial cells after OGD treatment *in-vitro*. Similarly, low expression of c-Myb also triggered a significant decrease in the expressions of cardiac fibrosis mark-

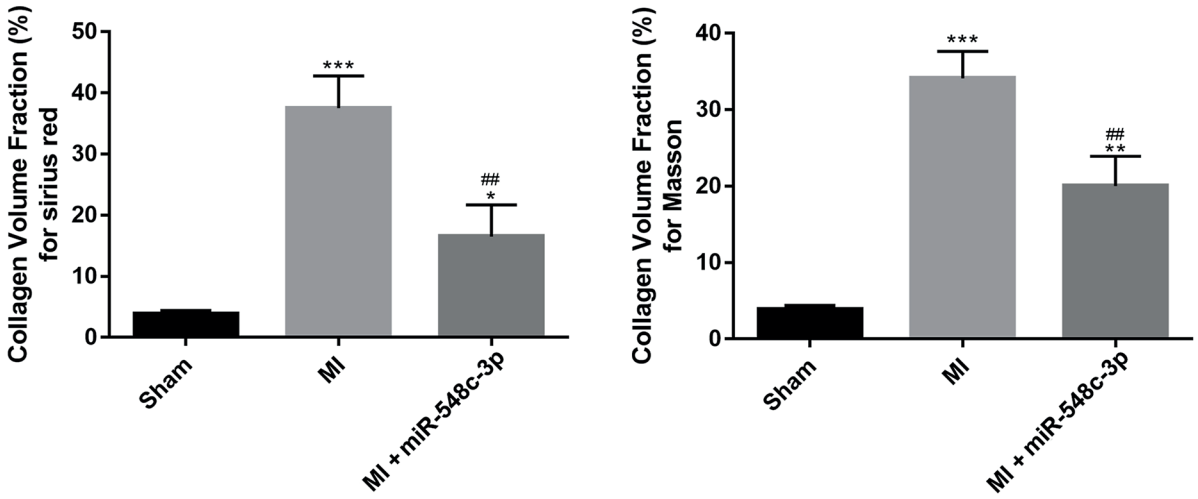

Figure 4. Collagen volume fraction determined by Sirius red and Masson staining. (*p<0.05, **p <0.01, ***p<0.001 compared with Sham group, ##p<0.01 *vs.* MI group).

er proteins (including α-SMA and COL1A1) in cardiomyocytes after OGD treatment (Figure 6).

Discussion

Myocardial fibrosis refers to the pathological process of excessive accumulation of extracellular matrix, significant increase in collagen content and changes in collagen fiber composition. Myocardial fibrosis is also an important factor of ventricular remodeling, which may lead to decline in compliance and cardiac insufficiency[18]. The main pathological changes of myocardial fibrosis after MI include: (1) the activation, proliferation and transformation of fibroblasts into myofibroblasts expressing α-SMA caused by myocardial ischemia and necrosis, and (2) the synthesis and secretion of a large number of extracellular matrix proteins (such as COL1A1). Among the above molecules, the protein expression of α-SMA is the typical manifestation of fibroblast transformation

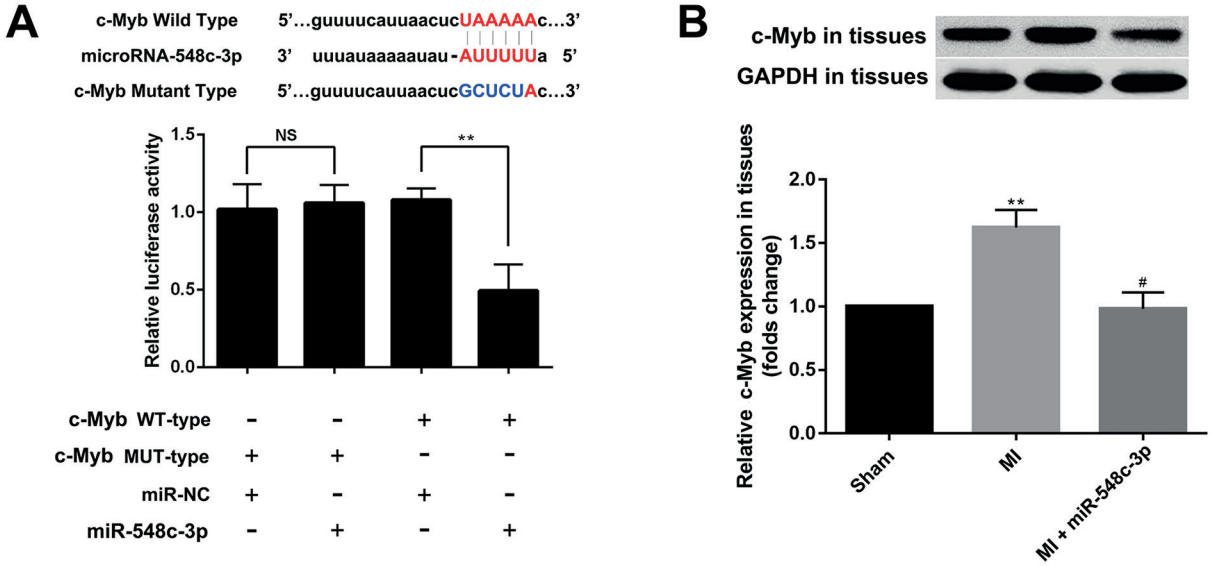

Figure 5. c-Myb was a direct and functional target of miR-548c-3p. ***A,*** Diagram of putative miR-548-3p binding sites of c-Myb and relative activities of luciferase reporters (**p<0.01). ***B,*** The protein expression of c-Myb in cardiac tissues after MI. (**p<0.01 compared with Sham group, #p<0.05 *vs.* MI group).

into myofibroblasts[18]. Therefore, cardiac function, collagen volume, α-SMA and COL1A1 expression are often indicators for myocardial fibrosis detection. C-Myb, as a nuclear transcription factor, has been proved to regulate tissue fibrosis through fibroblasts. For example, Ma et al[19] have found that down-regulation of c-Myb can inhibit hepatic stellate cell proliferation, and the expressions of COL1A1 and TGF-β expression, thereby suppressing liver fibrosis. Besides, Piccinini et al[20] have found that c-Myb can trans-activate human dermal fibroblast type I collagen-α2 precursor, thereby up-regulating type I collagen. Recent studies have also indicated that c-Myb activates the transformation of myocardial fibroblasts into myofibroblasts, eventually promoting COL1A1 and α-SMA expression[21]. According to a large number of studies, miRNAs play important regulatory roles in cardiovascular pathophysiological processes, including cardiac development, cardiac remodeling, arrhythmia, angiogenesis and vascular lesions. Studies have also found that the expressions of various miRNAs are significantly changed in MI region in animal models. VanRooij et al[22] detected miRNA expression in the marginal zone and remote zone of MI at 3 and 14 d after MI in rats. They have found that MI is accompanied by changes in miRNA expression, and such changes evolve with time. Therefore, it is speculated that the changes of these miRNAs are likely to be related with disease progression after MI. Moreover, Shan et al[23] have found that both miR-1 and miR-206 levels are continuously increased after MI at 1, 2 and 4 weeks, which reach peak at 4 weeks. In addition, miR-206 can also inhibit the expression of anti-apoptotic gene IGF-1 at the post-transcriptional level, thereby reducing anti-apoptotic effect on myocardial cells. Rane et al[24] have indicated that miR-199a rapidly declines 30 min after MI. This indicates that the changes in miRNA expression are diverse and complex during the development of MI. Wang et al[25] detected whole-genome miRNA expression in patients with acute MI using the peripheral blood samples for the first time. They have demonstrated that 121 miRNAs are abnormally regulated in patients with acute MI when compared with normal controls. Among all miRNAs, miR-1291 and miR-663b exhibited the highest sensitivity and specificity. Therefore, it is believed that some specific miRNAs extracted from peripheral blood are expected to serve as new markers for the diagnosis of MI. Similar conclusions have been made by Wang et al[25-27] in their study. Besides, Meder et al[28] have also found that the expression levels of miR-30c and miR-145 are closely associated with MI area. Another group has constructed the adenovirus vector over-expressing miR-21, and found that MI area declines by 29% within 24 h. Meanwhile, the left ventricular diameter becomes smaller within 2 weeks, confirming the intervention effect of miRNAs on MI[29].

In our study, the protective effect of miR-548c-3p on cardiac function after MI was excellent *in vivo*. Furthermore, we found that miR-548c-3p could not only stabilize the structural changes of myocardial tissue after MI, but also play an important role in anti-fibrosis. MiRNAs usually bind to the 3'-UTR of target mRNAs to induce mRNA degradation, thus inhibiting the expression of target genes[30]. According to bioinformatics analysis and luciferase reporter gene assay, c-Myb was predicted and confirmed as a direct target of miR-548c-3p. Our subsequent *in vitro* results revealed that high expression of miR-548c-3p in neonatal rat cardiac fibroblasts significantly inhibited the

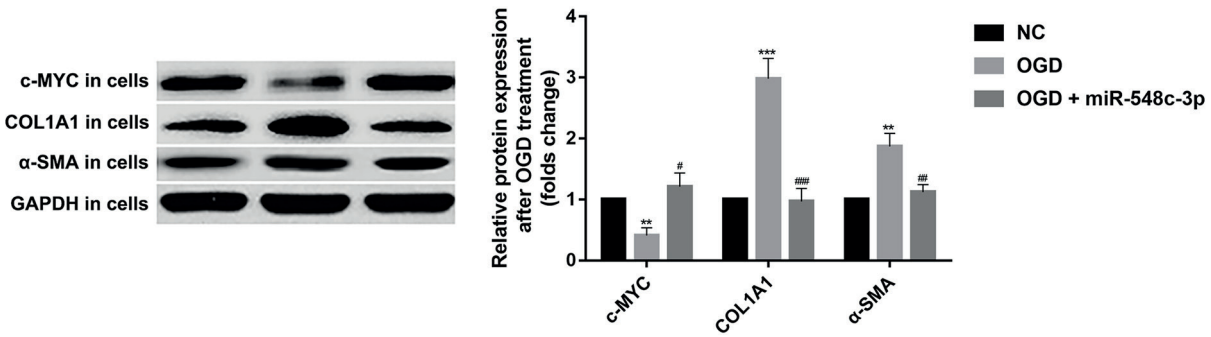

Figure 6. Up-regulation of miR-548c-3p inhibited the expressions of c-Myb and fibrosis-related factors (α-SMA and COL1A1) after OGD treatment. (***p*<0.01, ****p*<0.001 *vs.* NC group; #*p*<0.05, ##*p*<0.01, ###*p* <0.001 *vs.* Mimics group).

expression of fibrosis-related factors (α-SMA and COL1A1) after OGD treatment. This might explain the effect of miR-548c-3p on fibrosis *in vivo*.

Conclusions

We found that miR-548c-3p inhibited myocardial fibrosis after MI through targeting c-Myb, which might provide a new direction for the treatment of MI.

Conflict of Interests

The Authors declare that they have no conflict of interests

References

1) Pater C. The current status of primary prevention in coronary heart disease. Curr Control Trials Cardiovasc Med 2001; 2: 24-37.
2) Mozaffarian D, Benjamin EJ, Go AS, Arnett DK, Blaha MJ, Cushman M, Das SR, de Ferranti S, Despres JP, Fullerton HJ, Howard VJ, Huffman MD, Isasi CR, Jimenez MC, Judd SE, Kissela BM, Lichtman JH, Lisabeth LD, Liu S, Mackey RH, Magid DJ, McGuire DK, Mohler ER, Moy CS, Muntner P, Mussolino ME, Nasir K, Neumar RW, Nichol G, Palaniappan L, Pandey DK, Reeves MJ, Rodriguez CJ, Rosamond W, Sorlie PD, Stein J, Towfighi A, Turan TN, Virani SS, Woo D, Yeh RW, Turner MB. Executive summary: heart disease and stroke statistics--2016 update: a report from the American Heart Association. Circulation 2016; 133: 447-454.
3) Lin RC, Weeks KL, Gao XM, Williams RB, Bernardo BC, Kiriazis H, Matthews VB, Woodcock EA, Bouwman RD, Mollica JP, Speirs HJ, Dawes IW, Daly RJ, Shioi T, Izumo S, Febbraio MA, Du XJ, McMullen JR. PI3K(p110 alpha) protects against myocardial infarction-induced heart failure: identification of PI3K-regulated miRNA and mRNA. Arterioscler Thromb Vasc Biol 2010; 30: 724-732.
4) Gidlof O, van der Brug M, Ohman J, Gilje P, Olde B, Wahlestedt C, Erlinge D. Platelets activated during myocardial infarction release functional miRNA, which can be taken up by endothelial cells and regulate ICAM1 expression. Blood 2013; 121: 3908-3917, S1-S26.
5) Guo ML, Guo LL, Weng YQ. Implication of peripheral blood miRNA-124 in predicting acute myocardial infarction. Eur Rev Med Pharmacol Sci 2017; 21: 1054-1059.
6) Meder B, Keller A, Vogel B, Haas J, Sedaghat-Hamedani F, Kayvanpour E, Just S, Borries A, Rudloff J, Leidinger P, Meese E, Katus HA, Rottbauer W. MicroRNA signatures in total peripheral blood as novel biomarkers for acute myocardial infarction. Basic Res Cardiol 2011; 106: 13-23.
7) Bang C, Batkai S, Dangwal S, Gupta SK, Foinquinos A, Holzmann A, Just A, Remke J, Zimmer K, Zeug A, Ponimaskin E, Schmiedl A, Yin X, Mayr M, Halder R, Fischer A, Engelhardt S, Wei Y, Schober A, Fiedler J, Thum T. Cardiac fibroblast-derived microRNA passenger strand-enriched exosomes mediate cardiomyocyte hypertrophy. J Clin Invest 2014; 124: 2136-2146.
8) Jayawardena TM, Egemnazarov B, Finch EA, Zhang L, Payne JA, Pandya K, Zhang Z, Rosenberg P, Mirotsou M, Dzau VJ. MicroRNA-mediated *in vitro* and in vivo direct reprogramming of cardiac fibroblasts to cardiomyocytes. Circ Res 2012; 110: 1465-1473.
9) Abonnenc M, Nabeebaccus AA, Mayr U, Barallobre-Barreiro J, Dong X, Cuello F, Sur S, Drozdov I, Langley SR, Lu R, Stathopoulou K, Didangelos A, Yin X, Zimmermann WH, Shah AM, Zampetaki A, Mayr M. Extracellular matrix secretion by cardiac fibroblasts: role of microRNA-29b and microRNA-30c. Circ Res 2013; 113: 1138-1147.
10) Brennecke J, Hipfner DR, Stark A, Russell RB, Cohen SM. bantam encodes a developmentally regulated microRNA that controls cell proliferation and regulates the proapoptotic gene hid in Drosophila. Cell 2003; 113: 25-36.
11) Lewis BP, Shih IH, Jones-Rhoades MW, Bartel DP, Burge CB. Prediction of mammalian microRNA targets. Cell 2003; 115: 787-798.
12) Lu J, Zhang M, Yang X, Cui T, Dai J. MicroRNA-548c-3p inhibits T98G glioma cell proliferation and migration by downregulating c-Myb. Oncol Lett 2017; 13: 3866-3872.
13) Luo Z, Li D, Luo X, Li L, Gu S, Yu L, Ma Y. Decreased expression of miR-548c-3p in osteosarcoma contributes to cell proliferation via targeting ITGAV. Cancer Biother Radiopharm 2016; 31: 153-158.
14) Srikantan S, Abdelmohsen K, Lee EK, Tominaga K, Subaran SS, Kuwano Y, Kulshrestha R, Panchakshari R, Kim HH, Yang X, Martindale JL, Marasa BS, Kim MM, Werstо RP, Indig FE, Chowdhury D, Gorospe M. Translational control of TOP2A influences doxorubicin efficacy. Mol Cell Biol 2011; 31: 3790-3801.
15) Tormo E, Pineda B, Serna E, Guijarro A, Ribas G, Fores J, Chirivella E, Climent J, Lluch A, Eroles P. MicroRNA profile in response to doxorubicin treatment in breast cancer. J Cell Biochem 2015; 116: 2061-2073.
16) Dzikiewicz-Krawczyk A. MicroRNA polymorphisms as markers of risk, prognosis and treatment response in hematological malignancies. Crit Rev Oncol Hematol 2015; 93: 1-17.
17) Zhong H, Xin H, Wu LX, Zhu YZ. Salidroside attenuates apoptosis in ischemic cardiomyocytes: a mechanism through a mitochondria-dependent pathway. J Pharmacol Sci 2010; 114: 399-408.
18) Zhang S, Cui R. The targeted regulation of miR-26a on PTEN-PI3K/AKT signaling pathway in myocardial fibrosis after myocardial infarction. Eur Rev Med Pharmacol Sci 2018; 22: 523-531.
19) Ma HH, Yao JL, Li G, Yao CL, Chen XJ, Yang SJ. Effects of c-myb antisense RNA on TGF-beta1

and beta1-I collagen expression in cultured hepatic stellate cells. World J Gastroenterol 2004; 10: 3662-3665.

20) Piccinini G, Luchetti MM, Caniglia ML, Carossino AM, Montroni M, Introna M, Gabrielli A. c-myb proto-oncogene is expressed by quiescent scleroderma fibroblasts and, unlike B-myb gene, does not correlate with proliferation. J Invest Dermatol 1996; 106: 1281-1286.

21) Deng P, Chen L, Liu Z, Ye P, Wang S, Wu J, Yao Y, Sun Y, Huang X, Ren L, Zhang A, Wang K, Wu C, Yue Z, Xu X, Chen M. MicroRNA-150 inhibits the activation of cardiac fibroblasts by regulating c-Myb. Cell Physiol Biochem 2016; 38: 2103-2122.

22) van Rooij E, Sutherland LB, Thatcher JE, DiMaio JM, Naseem RH, Marshall WS, Hill JA, Olson EN. Dysregulation of microRNAs after myocardial infarction reveals a role of miR-29 in cardiac fibrosis. Proc Natl Acad Sci U S A 2008; 105: 13027-13032.

23) Shan ZX, Lin QX, Fu YH, Deng CY, Zhou ZL, Zhu JN, Liu XY, Zhang YY, Li Y, Lin SG, Yu XY. Upregulated expression of miR-1/miR-206 in a rat model of myocardial infarction. Biochem Biophys Res Commun 2009; 381: 597-601.

24) Rane S, He M, Sayed D, Vashistha H, Malhotra A, Sadoshima J, Vatner DE, Vatner SF, Abdellatif M. Downregulation of miR-199a derepresses hypoxia-inducible factor-1alpha and Sirtuin 1 and recapitulates hypoxia preconditioning in cardiac myocytes. Circ Res 2009; 104: 879-886.

25) Wang GK, Zhu JQ, Zhang JT, Li Q, Li Y, He J, Qin YW, Jing Q. Circulating microRNA: a novel potential biomarker for early diagnosis of acute myocardial infarction in humans. Eur Heart J 2010; 31: 659-666.

26) Cheng Y, Tan N, Yang J, Liu X, Cao X, He P, Dong X, Qin S, Zhang C. A translational study of circulating cell-free microRNA-1 in acute myocardial infarction. Clin Sci (Lond) 2010; 119: 87-95.

27) Ai J, Zhang R, Li Y, Pu J, Lu Y, Jiao J, Li K, Yu B, Li Z, Wang R, Wang L, Li Q, Wang N, Shan H, Li Z, Yang B. Circulating microRNA-1 as a potential novel biomarker for acute myocardial infarction. Biochem Biophys Res Commun 2010; 391: 73-77.

28) Meder B, Keller A, Vogel B, Haas J, Sedaghat-Hamedani F, Kayvanpour E, Just S, Borries A, Rudloff J, Leidinger P, Meese E, Katus HA, Rottbauer W. MicroRNA signatures in total peripheral blood as novel biomarkers for acute myocardial infarction. Basic Res Cardiol 2011; 106: 13-23.

29) Dong S, Cheng Y, Yang J, Li J, Liu X, Wang X, Wang D, Krall TJ, Delphin ES, Zhang C. MicroRNA expression signature and the role of microRNA-21 in the early phase of acute myocardial infarction. J Biol Chem 2009; 284: 29514-29525.

30) Bartel DP. MicroRNAs: genomics, biogenesis, mechanism, and function. Cell 2004; 116: 281-297.